Underactuated Soft Hip Exosuit Based on Adaptive Oscillators to Assist Human Locomotion

Enrica Tricomi[1*], Nicola Lotti[1], Francesco Missiroli[1], Xiaohui Zhang[1], Michele Xiloyannis[2], Thomas Müller[4] Simona Crea[3], Emese Papp[4], Jens Krzywinski[4], Nicola Vitiello[3], and Lorenzo Masia[1]

***Abstract*—Reproducing the mechanisms of human locomotion is a hard challenge. Assistive wearable devices in this context need to be lightweight, portable, and to adapt to the wearer's walking pattern. Aiming to combine the aforementioned features, we developed a soft wearable exosuit to assist hip flexion during walking. The main feature of the device is underactuation, i.e., a single actuator is used to assist bilateral hip flexion. A control strategy based on Adaptive Oscillators and gait phase estimation is implemented to deliver flexible assistance and to adapt to changes in walking pattern. The system was tested on six healthy subjects. Preliminary results show good performance of the control algorithm to track human gait and to deliver symmetrical assistance to both legs. First kinematic and muscular assessments revealed promising results at walking speeds near to the natural human walking, where the device did not alter hip kinematics and decreased the effort required by muscles contributing to hip flexion. Once validated on a larger sample of subjects, the device can have the potentialities to be used in clinical and wellness applications.**

***Index Terms*—Wearable Robotics; Modeling, Control, and Learning for Soft Robots; Underactuated Robots; Adaptive Oscillators; Gait Phase.**

I. Introduction

HUMAN locomotion is a complex mechanism, refined over three million years of evolution [1]. During the long and winding road of our life, this mechanism could be affected by degradation depending on several factors, such as traumatic events, neuromuscular diseases, or simply aging. One way to restore such motor functions foresees the assistance of rigid wearable robots to replace the structural and actuation properties of the human body, i.e., rigid exoskeletons [2], [3]. This method proved tangible efficacy both on severely impaired subjects and in individuals affected by mild conditions [4].

Manuscript received: September, 8^{th}, 2020; Revised November, 22^{th}, 2020; Accepted December, 9^{th}, 2020.

This paper was recommended for publication by Editor Jee-Hwan Ryu upon evaluation of the Associate Editor and Reviewers' comments. This work was supported by the project HeiAge and SMART-AGE (Project No.: P2019-01-003) by Carl Zeiss Foundation.

[1] Enrica Tricomi, Nicola Lotti, Francesco Missiroli, Xiaohui Zhang, and Lorenzo Masia are with the Institut für Technische Informatik (ZITI), Heidelberg University, 69120 Heidelberg, Deutschland.

[2]Michele Xiloyannis is with the Institute of Robotics and Intelligent Systems, ETH Zürich, Zürich, 8092, Switzerland.

[3]Simona Crea and Nicola Vitiello are with the BioRobotics Institute, Scuola Superiore Sant'Anna, 56127 Pisa, Italy, with the Department of Excellence in Robotics and AI, Scuola Superiore Sant'Anna, 56127 Pisa, Italy, and with the IRCCS Fondazione Don Carlo Gnocchi ONLUS, 50143, Florence, Italy.

[4]Thomas Müller, Emese Papp, and Jens Krzywinski are with the Chair of Industrial Design Engineering, Technische Universität Dresden, 01062 Dresden, Deutschland.

∗ corresponding author: enrica.tricomi@ziti.uni-heidelberg.de

Digital Object Identifier (DOI): see top of this page.

In parallel to traditional exoskeletons, the recent development of lightweight wearable robots, designed as clothing-like devices, demonstrated to be a valid alternative to restore movement abilities. These robots, namely soft "exosuits", are mainly made of textile frames able to adapt to users' body shape, being noteworthy for their portability and low weight [5], [6]. These features allow preventing kinematic restrictions, preserving natural gait biomechanics, while providing assistive forces at specific times along the walking cycle [7].

In the current state of the art, most of the aforementioned devices present one actuator for each degree of freedom (DoF) of the targeted joint. This allows for full assistance modulation of single movements but suffers from poor scalability of system complexity and weight. However, in the context of human motor coordination, studies have shown that the broad set of limb movements can be achieved through simplified control strategies, which imply the synergistic activation of different muscles [8], [9]. This concept has inspired new robotic hands design principles that use a smaller number of independent actuators than controlled joints, whose synchronous activation can provide different hand movements and postures [10], [11]. Compared to 1 actuator-1 DoF solutions, these devices stand out for reduced weight, and simpler mechanical and control designs [12].

Although several attempts were done in introducing underactuation on upper-limb robotic devices, very few examples exist for lower-limb solutions [13], [14]. This comes from the high redundancy in the involvement of muscles to perform upper-limb movements, which action can be more easily combined. Instead, in the lower-limbs, given the cyclic nature of gait patterns, underactuation principles should be complemented with suitable control strategies to prevent movement hindering. To act consistently with the natural gait, it becomes crucial to detect the phase of the intended movement in real-time and to adapt to perturbations [15].

From the control strategy viewpoint, among the techniques present in literature, recent interest focused on Adaptive Oscillators (AOs) [16], [17]. AOs can be described as a mathematical tool able to synchronize with a rhythmic and periodic signal by continuously estimating its fundamental features (i.e. frequency, amplitude, phase, and offset). For their properties, AOs found applications in gait pattern estimation strategies, where they are used to mimic the dynamics of the neuromechanical oscillators in charge of the rhythmical human locomotion. In addition, as gait periodicity can be captured by sensors recording joint kinematics, their application does not require a complex sensory network.

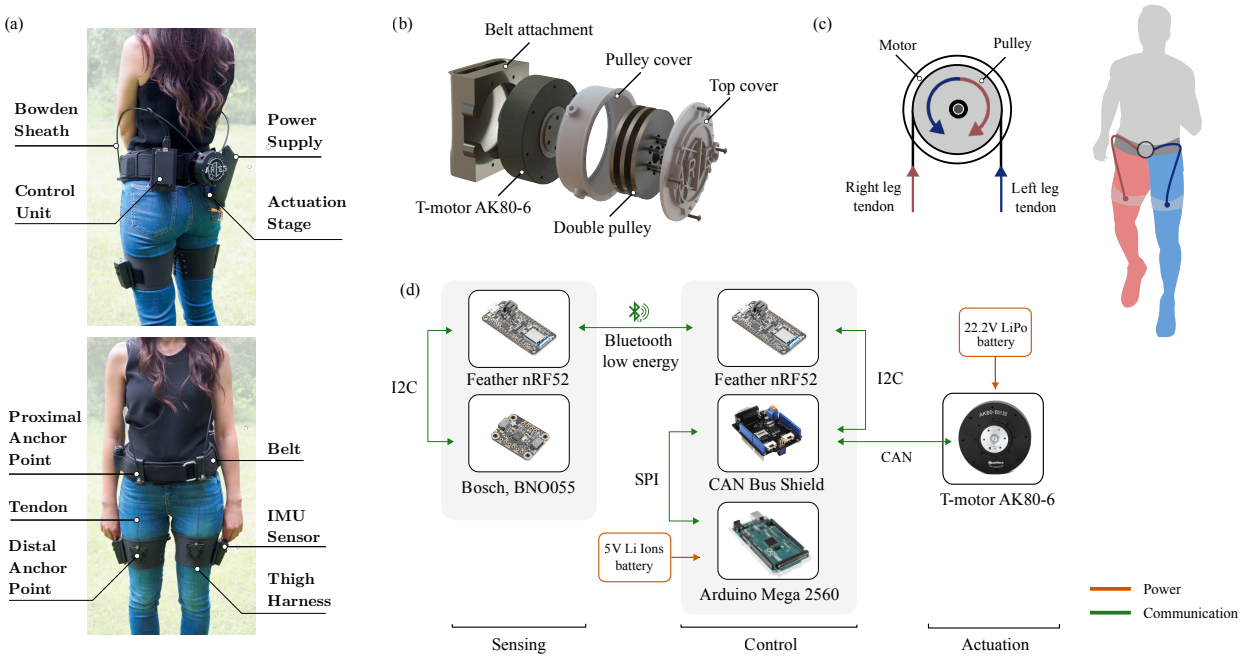

Fig. 1. *Hip Exosuit design and actuation principles.* (a) The exosuit is made of a lightweight belt hosting the actuation stage, control unit, and power supply, and two fabric harnesses on the thighs. Two artificial tendons assist the user by moving closer the proximal and distal anchor points. The sensing unit is composed of two IMUs placed at the thigh level that record the hip flexion angle. (b-c) The actuation stage is made of one brushless DC motor with a double-layer pulley that wraps up the left and right leg tendons in opposite direction: when one is pulled, the other is released. (d) Hardware exosuit design. The control unit comprises an Arduino Mega 2560 communicating with the motor via CAN Bus and with the sensing unit via BLE.

To combine simplicity, lightweight, and adaptive assistance features, we developed a fully embedded undearctuated wearable system and tested it to assist hip flexion during walking. The primary objective of this work is to advance an underactuated soft design to assist human locomotion (i.e., the use of a single actuator to assist both legs), supported by the periodicity of human walking and the phase shift between the gait states at the two legs. Simplicity and lightweight properties are also addressed by the sensory apparatus of the device, solely based on Inertial Measurement Unit (IMU) sensors used to detect the flexion angle at the hip joint. For a flexible and adaptive assistance delivered to the user, we incorporated the gait phase estimator algorithm presented in Yan et al. [15], opportunely implemented to drive an underactuated system. The algorithm is based on Adaptive Oscillators (AOs) to learn online the frequency, amplitude, and phase components of the hip flexion trajectories. The device was tested on a cohort of six healthy subjects on treadmill evaluations to preliminary assess its performance.

To our knowledge, this is the first time that a soft underactuated design based on AOs and complemented by a simple sensing system is presented to assist human walking.

II. Exosuit Design

The present underactuated exosuit has been designed to assist hip flexion during walking. The device has an overall weight of $2.2\,\mathrm{kg}$, it can provide up to 12 Nm peak torque for each leg, and it has an autonomy of $\approx 10\,\mathrm{h}$ of continuous operation. The system is completely embedded with a compact design and a wireless sensory network.

The textile frame is mainly made of two parts tightened to the user's body through Velcro® stripes and lacing systems (Fig. 1-a). The first main component is a lightweight belt (RDX Sport, Stafford, Texas, USA) wrapped around the user's waist and the second one comprises two soft fabric harnesses made of a double layer of Neoprene and Teflon placed around the thighs. The back of the belt hosts the actuation stage, the control unit, and the power supply.

The user is assisted through a pair of artificial tendons (Black Braided Kevlar Fiber, KT5703-06, $2.2\,\mathrm{kN}$ max load, Loma Linda CA, USA) running from the actuation stage to the front of the device and anchored to the wearer's thighs. A Bowden sheath (Shimano SLR, $\varnothing 4\,\mathrm{mm}$, Sakai, Ōsaka, Japan) covers each tendon from the motor to the proximal anchor points: these are hook-shaped 3D printed components placed on the anterior part of the belt at the level of the iliac crest. The uncovered part of the artificial tendons runs parallel to the wearer's thigh and connects to the distal anchor points, consisting of 3D printed components sewed on the frontal part of the thigh harnesses. To assist the user, the actuator tensions the tendon by moving the two anchor points closer, applying a flexing moment at the hip joint.

The actuation stage (Fig. 1-b) is composed of (1) a single brushless DC motor (AK80-6, 6:1 gear reduction, Cube Mars actuator, T-MOTOR, Nanchang, Jiangxi, China), and (2) a double-layer pulley ($\varnothing 78\mathrm{mm}$) mounted on the motor. Each layer of the pulley wraps up the right and left leg cables in two different directions (clockwise and counterclockwise, respectively). Motor rotation pulls one cable and releases the other according to the wearer's motion (Fig. 1-c).

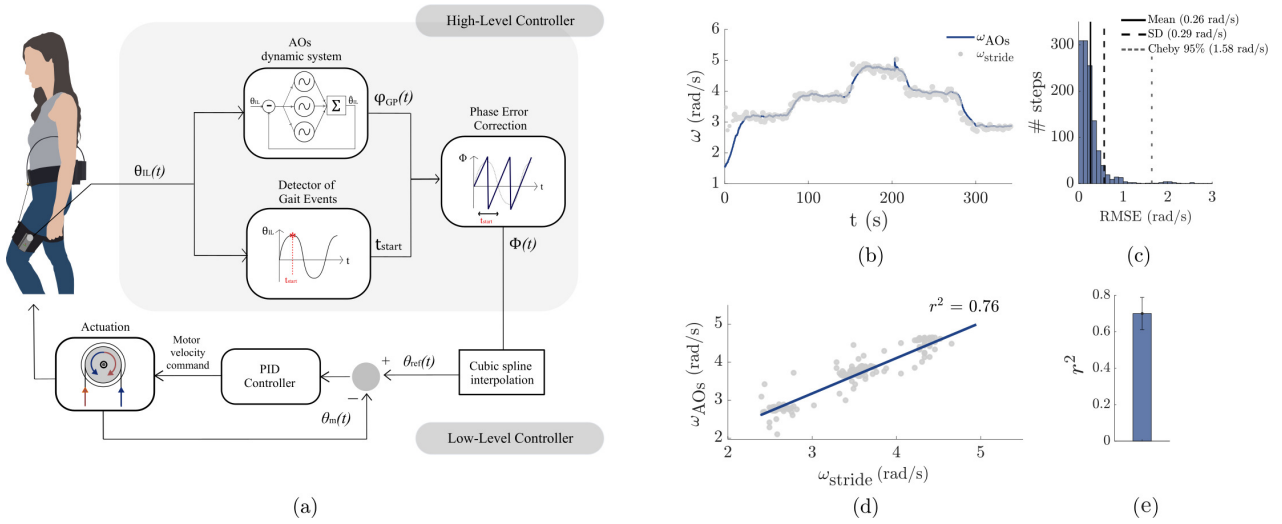

Fig. 2. *AOs-based Control Scheme and Performance Assessment*. (a) The control framework comprises a High-Level and a Low-Level Controller. The High-Level estimates the gait phase $\varphi_{\text{GP}}(t)$ by tracking the inter-limb hip flexion angle $\theta_{\text{IL}}(t)$ with Adaptive Oscillators (AOs dynamic system module). $\varphi_{\text{GP}}(t)$ is then corrected (Phase Error Correction module) according to each stride initiation (Detector of Gait Events module). The Low-Level converts the corrected gait phase $\phi(t)$ to a motor reference motion $\theta_{\text{ref}}(t)$ through cubic spline interpolation, then compared to the motor actual position $\theta_{\text{m}}(t)$. The position error ($\theta_{\text{ref}} - \theta_{\text{m}}$) is converted to motor angular velocity via PID. (b) Walking angular frequency estimated by AOs (ω_{AOs}) and measured angular frequency (ω_{stride}) in the variable walking speed task of a typical subject. (c) RMSE distribution between ω_{AOs} and ω_{stride} of each cycle of all subjects. Black solid line is the mean RMSE; black dashed line is the SD; grey dotted line is the maximal expected error within the 95th percentile of the data (Cheby 95%). (d-e) Angular frequency tracking accuracy of a typical subject and the mean coefficient of determination (r^2) among subjects.

The sensor unit is composed of two IMUs (Bosch, BNO055, Gerlingen, Germany) mounted laterally on the thigh harnesses, aiming to record the hip joint kinematics. IMU sensors communicate with the control unit via Bluetooth Low Energy (BLE) serial protocol through a microcontroller (Feather nRF52 Bluefruit, Adafruit Industries, New York City, USA). Data from IMUs (9-axis measurements of accelerometer, gyroscope, and magnetometer) are merged with the nine DoFs fusion mode of the sensor and extracted in form of quaternions to get the femur inclination with respect to the vertical axis. This angle can be a good approximation of the hip flexion angle if the trunk is in the upright posture.

The control framework runs on an Arduino® Mega 2560 (Arduino, Ivrea (TO), Italy) at 100 Hz, which sends commands to the actuation stage via CAN Bus (Fig. 1-d).

III. Real-Time Control Framework

The real-time control framework includes two layers (Fig. 2-a): a High-Level Controller, estimating the gait phase by tracking the hip flexion angle through AOs [16], and a Low-Level controller, which provides the needed assistance to both legs according to the motion.

A. High-Level Controller: Gait Phase Estimator

The High-Level Controller estimates the gait phase in real-time from kinematic data (i.e., hip flexion angles) through the AOs approach: this framework is called Gait Phase Estimator and it has been adapted from Yan et al. [15].

The Gait Phase Estimator has three main modules: the AOs dynamic system, the Detector of Gait Events, and the Phase Error Correction, which are detailed in sections III-A1 to III-A3. In our controller, the structure described in [15] has been adapted to comply with an underactuated system: hence, in our device, the driving signal is the inter-limb angle $\theta_{\text{IL}}(t)$ obtained as the difference between right and left hip angular displacement. Assistance is provided to each leg only during swing, while no assistive forces are applied during stances.

1) AOs dynamic system: The first module is a dynamic system based on AOs that estimates the inter-limb hip flexion angle $\theta_{\text{IL}}(t)$ as sum of sinusoidal functions:

$$\hat{\theta}_{\text{IL}}(t) = \alpha_0(t) + \sum_{n=1}^{N} \alpha_{\text{n}}(t)\sin(\varphi_{\text{n}}(t)) \tag{1}$$

with $\hat{\theta}_{\text{IL}}(t)$ the reconstructed input signal, $\alpha_{\text{n}}(t)$ and $\varphi_{\text{n}}(t)$ amplitude and phase of each harmonic, and $\alpha_0(t)$ the offset.

Specifically, signal characteristics are obtained integrating the following equations [16]:

$$\dot{\varphi}_{\text{n}}(t) = \omega(t)\cdot n + \nu_{\varphi}\frac{F(t)}{\sum \alpha_{\text{n}}}\cos(\varphi_{\text{n}}(t)) \tag{2}$$

$$\dot{\omega}(t) = \nu_{\omega}\frac{F(t)}{\sum \alpha_n}\cos(\varphi_1(t)) \tag{3}$$

$$\dot{\alpha}_{\text{n}}(t) = \eta F(t)\sin(\varphi_{\text{n}}(t)) \tag{4}$$

$$\dot{\alpha}_0(t) = \eta F(t) \tag{5}$$

where $F(t) = \theta_{\text{IL}}(t) - \hat{\theta}_{\text{IL}}(t)$ is the driving signal determining the convergence of each variable to the input, $\omega(t)$ is the fundamental frequency, and ν_{φ}, ν_{ω} and η are gains determining respectively the learning speeds of phase, frequency, and amplitude. We set the number of harmonics to $N = 3$, as suggested in [15] to track human walking biomechanics, while learning gains were tuned from offline preliminary trials and set to $\nu_{\varphi} = 20$, $\nu_{\omega} = 20$, and $\eta = 5$.

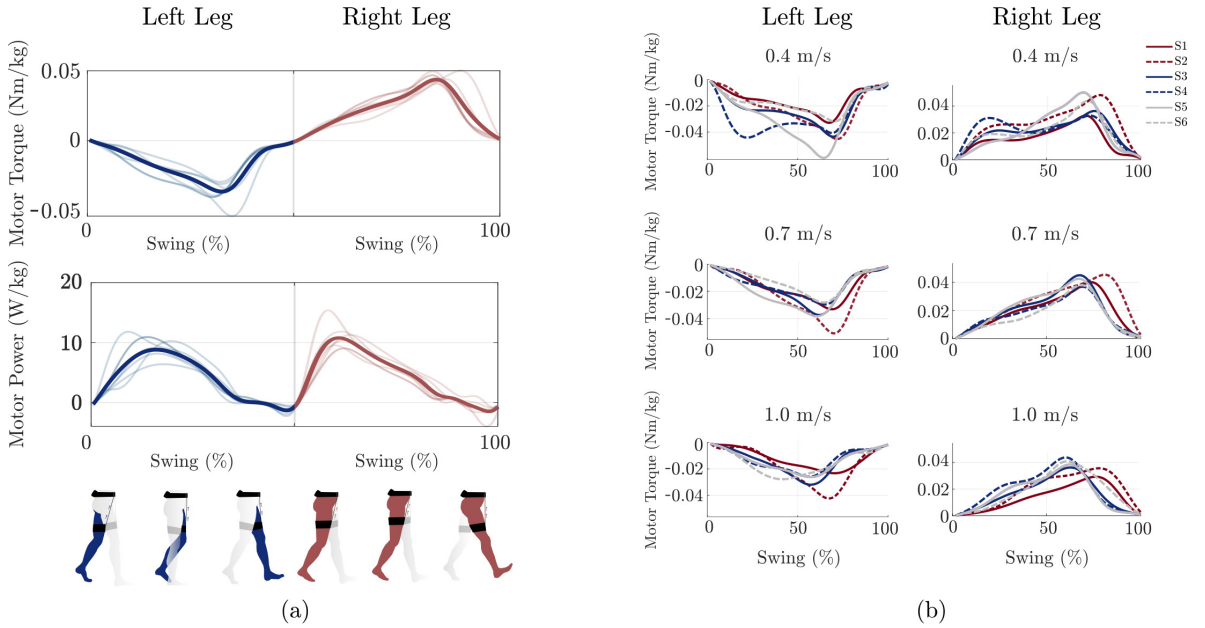

Fig. 3. *Motor torque and power analysis*. (a) Motor torque and power profiles at 0.7 m/s. A whole gait cycle is shown: negative torque values refer to assistance to the left leg (in blue); positive torque values to assistance to the right leg (in red). Thin transparent lines are the mean gait cycles in 3 minutes walking for each subject; the thick line is the mean across subjects. (b) Motor torque profiles for the trials at constant walking speed (0.4 m/s, 0.7 m/s, 1.0 m/s). Data are shown separately for the left and right leg. Each line represents the mean gait cycle during 3 minutes walking for each subject.

From AOs, the fundamental phase (namely $\varphi_1(t)$) is normalized in the interval $[0, 2\pi)$ to obtain a continuous gait phase variable $\varphi_{GP}(t)$ varying from 0 to 2π along a stride:

$$\varphi_{\text{GP}}(t) = \text{mod}(\varphi_1(t), 2\pi) \tag{6}$$

2) Detector of Gait Events: This module identifies the beginning of each gait cycle. From $\theta_{\text{IL}}(t)$, gait events indicating the beginning of a stride were recorded as the moment of maximum hip flexion. These instants, t_{i}, were found as the times in which the hip angular velocity crosses the zero.

To reject wrong detections, each selected time t_{i} is considered as a real start (t_{start}) if it is distant from the last detected time at least 0.7 times the stride period $T(t)$. In our application, this threshold showed good results in preliminary tests. Each stride period is computed as $T(t) = 2\pi/\omega(t)$, where $\omega(t)$ is estimated from the AOs module.

3) Phase Error Correction: The last module of the Gait Phase Estimator takes care of aligning the gait phase variable (i.e., $\varphi_{\text{GP}}(t)$) obtained from AOs with each t_{start}. In each gait cycle, $\varphi_{\text{GP}}(t)$ linearly increases from 0 to 2π rad, where 0 rad should correspond to a detected gait event. The potential mismatch and its variation along the gait cycle is corrected through the computation of the following variable:

$$\dot{\varphi}_{\text{e}} = C_{\text{e}}\omega(t)e^{-\omega(t)(t-t_{\text{start}})} \tag{7}$$

where $C_{\text{e}} = k_{\text{e}}(P_{\text{e}}(t_{\text{start}}) - \varphi_{\text{e}}(t_{\text{start}}))$ is a proportional gain determining the error at t_{start}, with k_{e} a constant gain (set to 1 from initial trials), $\omega(t)$ the AOs fundamental frequency, and $P_{\text{e}}(t_{\text{start}})$ the mismatch between the desired gait event and the gait phase $\varphi_{\text{GP}}(t)$. $P_{\text{e}}(t_{\text{start}})$ is computed as follows:

$$P_{\text{e}}(t_{\text{start}}) = \begin{cases} -\varphi_{\text{GP}}(t_{\text{start}}), & \text{if } 0 \leq \varphi_{\text{GP}}(t_{\text{start}}) < \pi \\ 2\pi - \varphi_{\text{GP}}(t_{\text{start}}), & \text{if } \pi \leq \varphi_{\text{GP}}(t_{\text{start}}) < 2\pi \end{cases} \tag{8}$$

The final gait phase $\phi(t)$ is computed by normalizing $\varphi_{\text{GP}}(t)$ in the interval $[0, 2\pi)$ after correction of the gait phase error:

$$\phi(t) = \text{mod}(\varphi_{\text{GP}}(t) + \varphi_{\text{e}}(t), 2\pi) \tag{9}$$

B. Low-Level Controller

The gait phase $\phi(t)$ obtained from the High-Level is further manipulated to obtain the desired input to the Low-Level, which outputs a velocity command to the motor.

We implemented the Low-Level controller as a feedback position loop that compares the position of the motor θ_{m} with a reference position θ_{ref}. To compute θ_{ref} we firstly shifted the gait phase obtained at the High-Level of π, then given as argument to a sinusoidal function:

$$\theta_{\text{r}} = \sin(\phi(t) - \pi) \tag{10}$$

We obtained the final θ_{ref} through cubic spline interpolation of θ_{r}. To convert the position error ($\theta_{\text{ref}} - \theta_{\text{m}}$) into motor angular velocity, we used a Proportional-Integral-Differential (PID) controller having transfer function:

$$Y(s) = \frac{K_p + K_i \cdot \frac{1}{s}}{1 + K_d \cdot s} \tag{11}$$

where the gains K_p, K_i, and K_d were tuned from preliminary trials to accurately follow the desired position θ_{ref}.

IV. Experiment

A. Experimental Setup

The effect of the device on muscular effort was evaluated using a multi-channel surface EMG system (Trigno wireless, Delsys, Natick MA, USA). Electrodes were placed according to the SENIAM guidelines [18]. We recorded muscle activity from two muscles contributing to hip flexion and extension, respectively Tensor Fasciae Latae (TFL) and Semitendinosus (ST), chosen according to electrode placement accessibility given by the device. Additionally, we monitored Tibialis Anterior (TA) and Gastrocnemius Lateralis (GL) activity to assess the effect on unassisted joints.

All signals were recorded through a DAQ board (Quanser QPIDe, Markham, Ontario, Canada) at 1 kHz. The real-time control was implemented in MATLAB/Simulink.

B. Experimental Protocol

To test our underactuated system, we enrolled six healthy subjects (four females/two males, age 27.14±1.86 years, mean±SD, weight 67.29±15.37 kg, height 172.14±12.40 cm). All participants had no history of musculoskeletal or neurological diseases. Before beginning the experiments all participants signed informed consent forms. Research procedures were performed in accordance with the Declaration of Helsinki and were approved by the Ethical Committee of Heidelberg University (resolution S-313/2020).

Subjects were requested to perform two different kinds of tasks consisting in walking on an actuated treadmill (Merax, G500) with (1) variable and (2) constant walking speed.

1) Variable walking speed: This task was designed to test the performance of the control algorithm to follow the user's motion intention and to adapt to new walking patterns. Subjects performed treadmill walking for a total of $5\,\mathrm{min}$, changing the speed from $0.4\,\mathrm{m/s}$, to $0.7\,\mathrm{m/s}$, to $1.0\,\mathrm{m/s}$, and back after $1\,\mathrm{min}$ intervals. This task was accomplished wearing the device and receiving assistance from the system.

2) Constant walking speed: This task aimed to assess the delivered assistance, effects on hip kinematics and EMG activity. It consisted of three trials at three different speeds ($0.4\,\mathrm{m/s}$, $0.7\,\mathrm{m/s}$, and $1.0\,\mathrm{m/s}$), lasting $5\,\mathrm{min}$ each. Each trial was repeated twice: with and without assistance. The assistance condition is indicated with the acronym "AOs" to relate to the AOs-based control approach; the no assistance condition is indicated with "NA". In the NA condition, the user still wore the exosuit, yet the power supply was switched off and tendons were untied from the distal anchor points.

Between trials, participants rested for $10\,\mathrm{min}$ to avoid the effect of fatigue. The order of tasks and trials, as well as AOs and NA conditions, was randomized across subjects.

Before each experimental session, we recorded the Maximum Voluntary Contraction (MVC) for each muscle, used to normalize EMG signals for the offline data analysis.

C. Data Analysis

1) Variable walking speed: The performance of the controller to adapt to users' walking pattern is mainly determined by a good tracking from AOs of the actual angular frequency of walking. Therefore, we compared the walking angular frequency estimated by AOs, ω_{AOs}, with the angular frequency measured at the hip joint through IMU sensors, ω_{stride}.

Raw kinematic data from IMUs (i.e., inter-limb hip flexion angle θ_{IL}) were low-pass filtered at $10\,\mathrm{Hz}$ (4^{th} order Butterworth filter) and segmented according to the different strides. Each stride was identified as the union of a positive and negative excursion in θ_{IL}, being this the difference between the right and left angular displacement. After segmentation, we computed the measured angular frequency as $\omega_{\text{stride}_\text{i}} = 2\pi/T_\text{i}$, with T_i the period of the i^{th} stride.

We quantified the error between ω_{AOs} and ω_{stride} by computing the Root Mean Square Error (RMSE) at each stride. To investigate the overall tracking accuracy, the coefficient of determination (r^2) was computed between ω_{stride} and ω_{AOs}.

2) Constant walking speed: Data from the constant speed task were analyzed to assess the delivered assistance, and effects on kinematics and muscular activity. From each $5\,\mathrm{min}$ recordings, we excluded the first and last minutes to avoid bias linked to the beginning and end of trials.

To assess the bilateral assistance provided by the underactu-

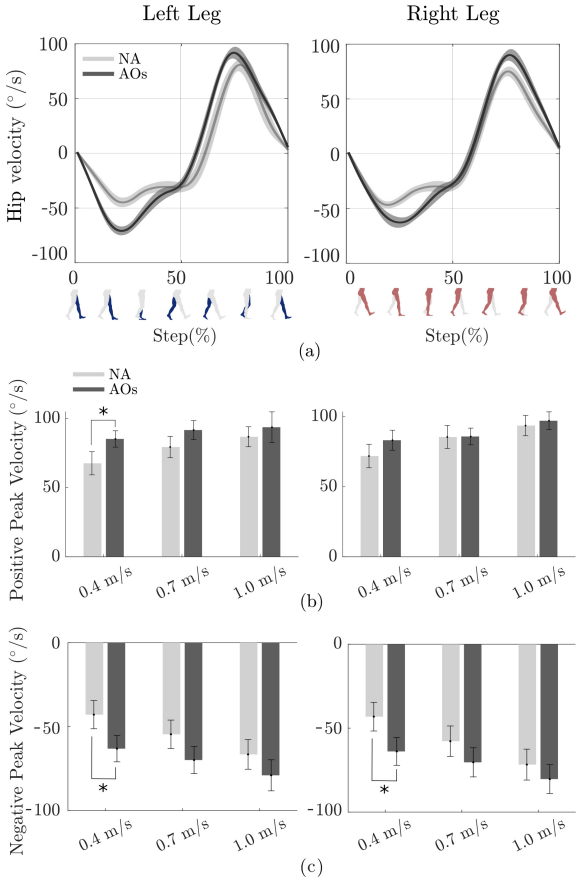

Fig. 4. *Kinematic Evaluation*. (a) Hip velocity profiles in percentage of step duration of both legs at $0.7\,\mathrm{m/s}$ of a typical subject, for NA (light gray) and AOs (dark grey) conditions. Solid line is the mean among steps in $3\,\mathrm{min}$ walking; shaded areas are the SD. (b-c) Positive peak (swing phase) and negative peak (stance phase) hip velocities averaged across subjects for the NA and AOs conditions at the three constant speed trials ($*$ indicates a statistical significant difference between conditions with $p<0.05$).

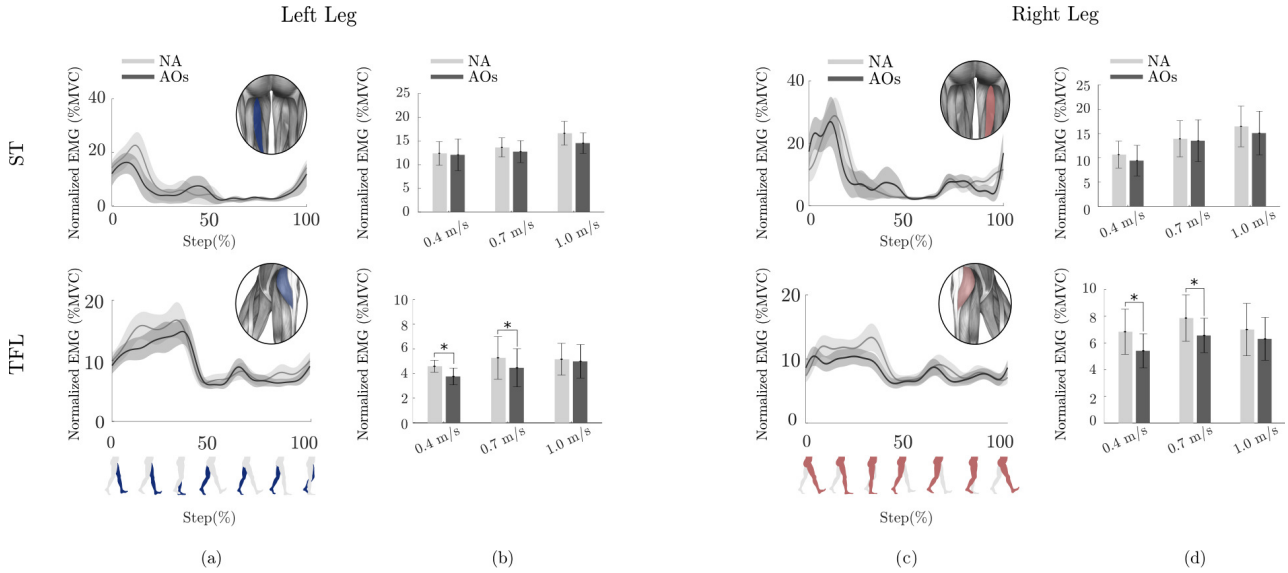

Fig. 5. *Effects on Muscular Activity*. (a-c) EMG envelopes of Semitendinosus (ST, top row) and Tensor Fasciae Latae (TFL, bottom row) muscles of both legs of a typical subject at $0.7\,\mathrm{m/s}$. Light grey curves show data for the NA condition; dark grey curves for the AOs condition. Solid lines is the mean among steps in $3\,\mathrm{min}$ walking; shaded areas is the SD. Data are presented in percentage of step duration. (b-d) Muscle activation (RMS) averaged across subjects for the NA and AOs conditions and the three constant speed trials ($*$ indicates a statistical significant difference between conditions with $p<0.05$).

ation mechanism, we evaluated the torque and power profiles at the motor during the swing phases of each leg. Raw motor torque data were low-pass filtered (4^{th} order Butterworth, cut-off frequency $10\,\mathrm{Hz}$), normalized with respect to subjects' weight, and segmented into the swing phases of each leg. Motor power was obtained by multiplying the normalized torque and motor angular velocity data.

The kinematic evaluation was performed on hip trajectories of the left and right leg independently. Raw IMU data were segmented into steps after low-pass filtering (4^{th} order Butterworth, cut-off frequency $10\,\mathrm{Hz}$). Gait was segmented according to hip angular velocity, obtained through a Savitsky-Golay filter. For each subject, we assessed the mean peak velocity in stance (negative peak) and swing (positive peak) across all steps in the NA and AOs conditions.

To assess muscular effects, we evaluated the change in muscle activation between NA and AOs conditions. EMG raw signals were band-pass filtered (20-400 Hz, 4^{th} order Butterworth), full wave rectified, and low-pass filtered (6 Hz, 4^{th} order Butterworth) to extrapolate the EMG envelope. Signals were normalized to subjects' MVC and segmented according to kinematic data. As index of muscle activation, we computed the Root Mean Square (RMS) at each step. For each subject, RMS values were averaged across steps.

D. Statistical Analysis

Data distributions were checked for normality with a Shapiro-Wilk test with significance level $\alpha = 0.05$. The normality test showed that data fit the normality distribution.

For kinematics and EMG assessments, a two-way ANOVA of "condition" (AOs vs. NA) and "walking speed" ($0.4\,\mathrm{m/s}$, $0.7\,\mathrm{m/s}$, $1.0\,\mathrm{m/s}$) with repeated measures on speed was used to find significant differences in the assessed metrics, in both legs. If the case, post-hoc analysis with Fisher's LSD was applied to identify pairwise differences between conditions.

Data are presented as mean with standard error (SE) unless otherwise specified.

V. Results

A. AOs-based control performance assessment

Fig. 2-b reports the AOs estimated angular frequency, ω_{AOs}, and the measured angular frequency, ω_{stride}, of a representative subject in the variable walking speed task. The RMSE between the measured and estimated angular frequencies for each cycle of all subjects are shown in the histogram of Fig. 2-c: the mean RMSE, computed by averaging errors across strides and subjects, was $0.26\pm0.29\ \mathrm{rad/s}$ (mean$\pm$SD).

Fig. 2-d shows the fitting between the measured and estimated angular frequency for a representative subject. The coefficient of determination (r^2) resulted in a mean value across subjects of 0.70 ± 0.22 (Fig. 2-e).

B. Motor torque and power analysis

Mean motor torque and power along a stride are shown in Fig. 3-a for the $0.7\,\mathrm{m/s}$ trial, as a representation of the exosuit working principle. By design, negative torque values refer to assistance during the left leg swing, while positive torque values to assistance during the right leg swing. Fig. 3-b reports the mean motor torque profiles for each subject and constant speed trial, separately for the left and right legs.

We recorded mean motor torque peak values across subjects of -0.042 ± 0.004 and 0.042 ± 0.004 Nm/kg (left and right respectively) in the $0.4\,\mathrm{m/s}$ trial; -0.037 ± 0.004 and 0.044 ± 0.002 Nm/kg in the $0.7\,\mathrm{m/s}$ trial; -0.029 ± 0.003 and $0.030\ \pm0.002$ Nm/kg in the $1.0\,\mathrm{m/s}$ trial.

C. Kinematic Evaluation

Fig. 4-a shows the hip velocity profiles at $0.7\,\mathrm{m/s}$ of a representative subject in the NA and AOs conditions. Comparing peak velocities reached during the three trials of the constant walking speed task, we found on average a slightly higher value in the AOs condition during the swing phase (positive peak) (Fig. 4-b) and a slightly lower value in the stance phase (negative peak) (Fig. 4-c). Yet, the two conditions resulted significantly different only at $0.4\,\mathrm{m/s}$ for the left leg in the swing phase (67.61$\pm$7.63; 85.20$\pm$6.50 $^\circ$/s, NA and AOs condition respectively) (p=0.004) and for both legs in the stance phase (p$<$0.005).

D. Effects on Muscular Activity

Results of the effects on muscular activity are depicted in Fig. 5 for the muscles contributing to hip flexion and extension, TFL and ST respectively. Panels a and c show the EMG envelopes of a representative subject averaged across steps at $0.7\,\mathrm{m/s}$, both in the NA and AOs conditions; panels b and d report the normalized RMS values averaged across subjects for the NA and AOs conditions and the three trials.

Wearing the exosuit significantly reduced the TFL activation at $0.4\,\mathrm{m/s}$, both for the left (p=0.02) and right leg (p=0.03). We recorded mean RMS values of 4.54$\pm$0.50 and 3.72$\pm$0.68 %MVC, NA and AOs respectively, for the left side; 6.85$\pm$1.70 and 5.42$\pm$1.28 %MVC for the right side.

The same trend was confirmed at $0.7\,\mathrm{m/s}$ for both legs (p=0.04). TFL activations for this trial were 5.21$\pm$1.70 and 4.41$\pm$1.53 %MVC, NA and AOs respectively, for the left leg; 7.88$\pm$1.74 and 6.57$\pm$1.29 %MVC for the right leg.

Results in TFL were not confirmed at higher walking speed ($1.0\,\mathrm{m/s}$) where the muscular effort was not significantly different between NA and AOs conditions.

Finally, no statistical difference was found between NA and AOs in all of the three trials for the muscle contributing to hip extension (SM, Fig. 5 top row), and for TA and GL.

VI. Discussion

Human walking does not only provide motion but it has been optimized during ages of evolution to deal with predictable and unpredictable interactions with the environment [19]. Assistive technologies should comply with these requirements without hampering natural movements; here is why the design and control of devices is such a challenge.

With the aim to assist human locomotion, we developed a fully portable wearable exosuit with an underactuated design for bilateral assistance. To mimic the periodicity of walking, we coupled the underactuation concept with an intuitive control strategy based on Adaptive Oscillators and gait phase estimation. The concept was tested on hip flexion assistance to primarily assess the feasibility of the proposed design.

Control performance showed reliable tracking of walking cadence with fast adaptability to new gait patterns. Specifically, we obtained a mean error of 0.26$\pm$0.29 $\mathrm{rad/s}$ between the AOs estimated walking frequency and the measured one (Fig. 2-c). Movement initiation from standstill required in general a higher number of steps to fully adapt (eight steps on average, consistently to [15]), while changes in gait cadence during the ongoing walking were rapidly matched (Fig. 2-b).

Assistance delivered to both legs resulted symmetrical in terms of motor torque and power profiles (Fig. 3). This is an encouraging result to prove the applicability of an underactuated system for bilateral assistance. Moreover, peak motor torque during swing resulted repeatable across subjects, hence indicating the potentialities of the device and adopted control scheme to deliver comparable assistive forces across different wearers and walking conditions.

Preliminary kinematic and muscular investigations showed good performance of the system at the intermediate tested speed ($0.7\,\mathrm{m/s}$) (Fig. 4-b-c, Fig. 5-b-d), where wearing the exosuit did not dramatically change joint kinematics and decreased muscle effort required for hip flexion by nearly 15%. Wearing the exosuit resulted in higher reductions in muscle activation (nearly 20%) at $0.4\,\mathrm{m/s}$ (Fig. 5-b-d), even though we found a significant increase of hip peak velocities in stance and swing (Fig. 4-b-c). The underlying reason is not clear: we may speculate that at this walking speed, being slower on average than natural human walking ($0.8-1.0\,\mathrm{m/s}$ [19]), subjects may have used assistance from the suit as a mean to compensate for the slowness of movement, whereas without assistance they were mostly guided by the speed imposed by the treadmill. Finally, at $1.0\,\mathrm{m/s}$ the system resulted transparent to the wearer in terms of kinematic evaluation. Wearing the exosuit did not significantly change muscle effort at this speed, although a small trend towards reduction in TFL activation can still be observed.

Regarding the limitations of our work, we assessed system performance in a limited range of walking speeds under controlled conditions (i.e., treadmill evaluations). Future studies will focus on different locomotion tasks and assess whether this design might hinder locomotion modes different from walking. As far as concern the effects on the user, we investigated these aspects at a very preliminary level. Kinematic assessments made use only of sensors mounted on the suit and need to be complemented with a more complex sensory equipment to study the effect on the whole lower limb kinematic chain. Moreover, device accessibility and artificial tendons position limited the possibility to complement the muscular investigations on the TFL muscle with other primary hip flexors (i.e. Rectus Femoris). However, given the correlated activity of both muscles, being main contributors to the targeted movement [20], we expect that our results may be easily transferred to other primary hip flexors. Future studies will combine in-depth kinematic, physiological, as well as metabolic consumption investigations.

As studies [21] proved that loading the wearer with external masses increases walking energetic cost, we expect that the low weight of our device and its close position to the user's center of mass will minimally impact energy consumption. Furthermore, since it has been shown [22], [23] that hip flexion assistive devices with negligible mass potentially provide substantial metabolic savings, we are confident that an improved design may lead to promising results in decreasing metabolic consumption on a variety of populations, ranging from elderly to mildly affected neurological patients.

In relation to other works, bilateral assistance through underactuation is a distinctive feature of our device. We believe that one of the main advantages introduced by such systems, coupled to adequate control strategies, is the possibility to reach high levels of balanced assistance delivered bilaterally. This has noteworthy repercussions on walking stability and motion regularity. Very few examples of similar kind are present in the literature so far and most of them make use of underactuation to synergistically assist multiple joints, still decoupling the two legs. To the best of our knowledge, only Panizzolo et al. developed a soft exosuit for underactuated bilateral assistance [13]. However, they incorporated two actuators in total to provide multi-joint assistance: one for bilateral hip flexion/ankle plantarflexion and the second one for bilateral hip extension. Compared to the aforementioned solution, our device assists a single DoF of one joint, yet our system is lighter (2.2kg vs. 6.6kg) and it integrates a control strategy able to adapt to the main features of human locomotion relying on a simple sensory network.

Given the encouraging preliminary results, we believe that our system can have good potentialities as an assistive technology for walking: the exosuit is extremely light and the modular composition makes donning and doffing procedures easy to the wearer. In addition, design compactness makes the system comfortable to the user that does not need to wear backpack-like hulking components similarly to most of the current existing solutions [5], [24]. These characteristics make the device suitable to target a wide range of users. Once validated on an larger sample of healthy individuals, device applicability can be extended to clinical applications in subjects with reduced motor performances or used as a well-being assistive technology by elderly people.

VII. Conclusions

In this study we presented a soft exosuit aimed to assist human locomotion making use of underactuation principles. An intuitive and adaptive control strategy based on Adaptive Oscillators has been implemented to provide assistance in relation to the gait phase and pattern. Results show that the device is able to reliably track human gait pattern and to provide similar assistance to both legs, even though it slightly alters human kinematic at the lowest speed, yet decreasing muscle effort. Outcomes of this preliminary investigation, as well as device lightweight and portability, support the idea that our soft exosuit could be a good candidate to assist human locomotion both for wellness and clinical purposes.

Acknowledgements

The results presented here have been obtained as part of the project HeiAge and SMART-AGE (Project No.: P2019-01-003) by Carl Zeiss Foundation.

References

[1] C. O. Lovejoy, "Evolution of human walking," *Scientific American*, vol. 259, no. 5, pp. 118–125, 1988.

[2] T. Lenzi, M. C. Carrozza, and S. K. Agrawal, "Powered hip exoskeletons can reduce the user's hip and ankle muscle activations during walking," *IEEE Transactions on Neural Systems and Rehabilitation Engineering*, vol. 21, no. 6, pp. 938–948, 2013.

[3] S. Wang, L. Wang, C. Meijneke, E. Van Asseldonk, T. Hoellinger, G. Cheron, Y. Ivanenko, V. La Scaleia, F. Sylos-Labini, M. Molinari *et al.*, "Design and control of the mindwalker exoskeleton," *IEEE transactions on neural systems and rehabilitation engineering*, vol. 23, no. 2, pp. 277–286, 2014.

[4] C. Hartigan, C. Kandilakis, S. Dalley, M. Clausen, E. Wilson, S. Morrison, S. Etheridge, and R. Farris, "Mobility outcomes following five training sessions with a powered exoskeleton," *Topics in spinal cord injury rehabilitation*, vol. 21, no. 2, pp. 93–99, 2015.

[5] A. T. Asbeck, S. M. De Rossi, K. G. Holt, and C. J. Walsh, "A biologically inspired soft exosuit for walking assistance," *The International Journal of Robotics Research*, vol. 34, no. 6, pp. 744–762, 2015.

[6] L. Chen, C. Chen, Z. Wang, X. Ye, Y. Liu, and X. Wu, "A novel lightweight wearable soft exosuit for reducing the metabolic rate and muscle fatigue," *Biosensors*, vol. 11, no. 7, p. 215, 2021.

[7] M. Xiloyannis, R. Alicea, A.-M. Georgarakis, F. L. Haufe, P. Wolf, L. Masia, and R. Riener, "Soft robotic suits: State of the art, core technologies, and open challenges," *IEEE Transactions on Robotics*, 2021.

[8] E. Bizzi, M. C. Tresch, P. Saltiel, and A. d'Avella, "New perspectives on spinal motor systems," *Nature Reviews Neuroscience*, vol. 1, no. 2, pp. 101–108, 2000.

[9] A. d'Avella, M. Giese, Y. P. Ivanenko, T. Schack, and T. Flash, "Modularity in motor control: from muscle synergies to cognitive action representation," *Frontiers in computational neuroscience*, vol. 9, p. 126, 2015.

[10] M. Santello, M. Bianchi, M. Gabiccini, E. Ricciardi, G. Salvietti, D. Prattichizzo, M. Ernst, A. Moscatelli, H. Jörntell, A. M. Kappers *et al.*, "Hand synergies: integration of robotics and neuroscience for understanding the control of biological and artificial hands," *Physics of life reviews*, vol. 17, pp. 1–23, 2016.

[11] D. Prattichizzo, M. Malvezzi, M. Gabiccini, and A. Bicchi, "On motion and force controllability of precision grasps with hands actuated by soft synergies," *IEEE transactions on robotics*, vol. 29, no. 6, pp. 1440–1456, 2013.

[12] C. Della Santina, C. Piazza, G. Grioli, M. G. Catalano, and A. Bicchi, "Toward dexterous manipulation with augmented adaptive synergies: The pisa/iit softhand 2," *IEEE Transactions on Robotics*, vol. 34, no. 5, pp. 1141–1156, 2018.

[13] F. A. Panizzolo, I. Galiana, A. T. Asbeck, C. Siviy, K. Schmidt, K. G. Holt, and C. J. Walsh, "A biologically-inspired multi-joint soft exosuit that can reduce the energy cost of loaded walking," *Journal of neuroengineering and rehabilitation*, vol. 13, no. 1, pp. 1–14, 2016.

[14] F. L. Haufe, K. Schmidt, J. E. Duarte, P. Wolf, R. Riener, and M. Xiloyannis, "Activity-based training with the myosuit: a safety and feasibility study across diverse gait disorders," *Journal of neuroengineering and rehabilitation*, vol. 17, no. 1, pp. 1–11, 2020.

[15] T. Yan, A. Parri, V. R. Garate, M. Cempini, R. Ronsse, and N. Vitiello, "An oscillator-based smooth real-time estimate of gait phase for wearable robotics," *Autonomous Robots*, vol. 41, no. 3, pp. 759–774, 2017.

[16] L. Righetti, J. Buchli, and A. J. Ijspeert, "Dynamic hebbian learning in adaptive frequency oscillators," *Physica D: Nonlinear Phenomena*, vol. 216, no. 2, pp. 269–281, 2006.

[17] ——, "Adaptive frequency oscillators and applications," *The Open Cybernetics & Systemics Journal*, vol. 3, no. 1, 2009.

[18] H. J. Hermens, B. Freriks, C. Disselhorst-Klug, and G. Rau, "Development of recommendations for semg sensors and sensor placement procedures," *Journal of electromyography and Kinesiology*, vol. 10, no. 5, pp. 361–374, 2000.

[19] D. A. Winter, *Biomechanics and motor control of human movement*. John Wiley & Sons, 2009.

[20] A. Hazari, A. G. Maiya, and T. V. Nagda, "Kinetics and kinematics of hip and pelvis," in *Conceptual Biomechanics and Kinesiology*. Springer, 2021, pp. 125–144.

[21] G. J. Bastien, P. A. Willems, B. Schepens, and N. C. Heglund, "Effect of load and speed on the energetic cost of human walking," *European journal of applied physiology*, vol. 94, no. 1, pp. 76–83, 2005.

[22] C. L. Dembia, A. Silder, T. K. Uchida, J. L. Hicks, and S. L. Delp, "Simulating ideal assistive devices to reduce the metabolic cost of walking with heavy loads," *PloS one*, vol. 12, no. 7, p. e0180320, 2017.

[23] F. A. Panizzolo, E. Annese, A. Paoli, and G. Marcolin, "A single assistive profile applied by a passive hip flexion device can reduce the energy cost of walking in older adults," *Applied Sciences*, vol. 11, no. 6, p. 2851, 2021.

[24] X. Wu, K. Fang, C. Chen, and Y. Zhang, "Development of a lower limb multi-joint assistance soft exosuit," *Science China Information Sciences*, vol. 63, pp. 1–3, 2020.